The University of Texas ARLINGTON

MATHEMATICS
Preprint Series

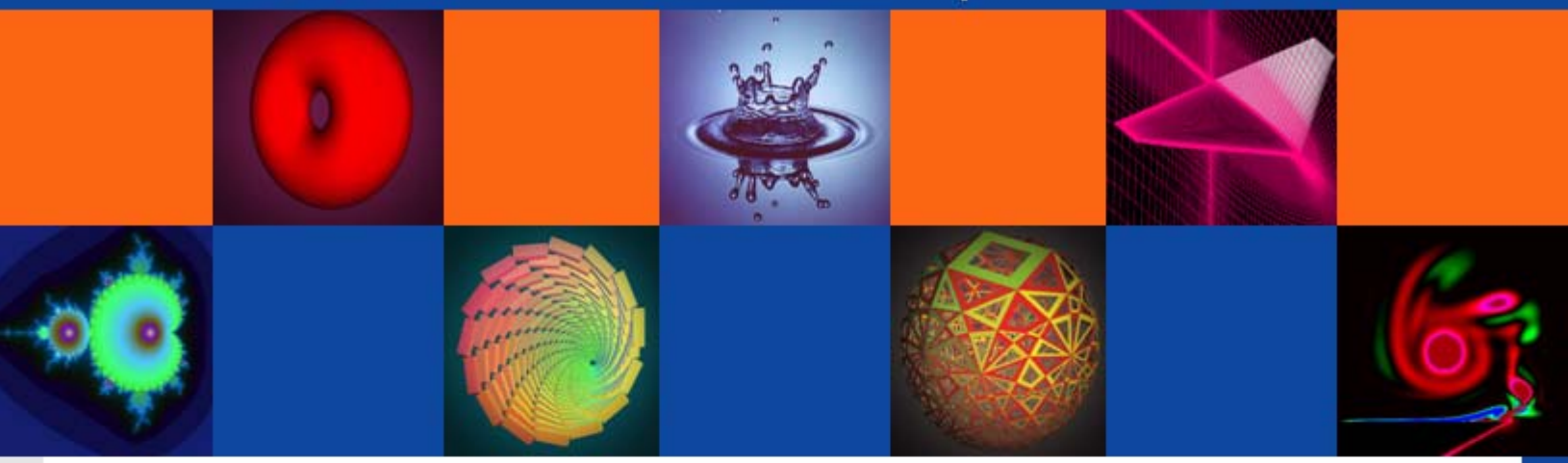

Solutions of Two-Factor Models With Variable Interest Rates

Jinglu Li, C.B. Clemons, G.W. Young, J. Zhu

Technical Report 2007-08

http://www.uta.edu/math/preprint/

Solutions of Two-Factor Models With Variable Interest Rates

Jinglu Li [a] C.B. Clemons [a] G.W. Young [a] J. Zhu [b,*]

[a] *Department of Theoretical and Applied Mathematics, The University of Akron, Akron, OH 44325–4002*

[b] *Department of Mathematics, The Univesity of Texas Arlingon, Arlington, TX 76019-0408*

Abstract

The focus of this work is on numerical solutions to two-factor option pricing partial differential equations with variable interest rates. Two interest rate models, the Vasicek model and the Cox-Ingersoll-Ross model (CIR), are considered. Emphasis is placed on the definition and implementation of boundary conditions for different portfolio models, and on appropriate truncation of the computational domain. An exact solution to the Vasicek model and an exact solution for the price of bonds convertible to stock at expiration under a stochastic interest rate are derived. The exact solutions are used to evaluate accuracy of the numerical simulation schemes. For the numerical simulations the pricing solution is analyzed as the market completeness decreases from the ideal complete level to one with higher volatility of the interest rate and a slower mean-reverting environment. Simulations indicate that the CIR model yields more reasonable results than the Vasicek model in a less complete market.

Key words: Two-factor models, variable interest rate, numerical simulation

1991 MSC: 35K99, 91B28, 35Q80,35Cxx, 65M06

1 Introduction

The focus of this work is on numerical solutions to two-factor option pricing partial differential equations with variable interest rates. Emphasis is placed

* Corresponding Author,Department of Mathematics, The Univesity of Texas Arlingon, Arlington, Tx 76019-0408. email:jpzhu@uta.edu

on the definition and implementation of boundary conditions on an appropriately truncated computational domain. For some limiting parameter ranges, basic exact solutions are derived and used to benchmark the accuracy of the numerical simulations.

Two interest rate models, the Vasicek model [11] and the Cox-Ingersoll-Ross model [5], are considered. To define the two-factor option pricing models, we follow the standard Black-Scholes model where the return on a portfolio Π earns the risk-less rate

$$d\Pi = r\Pi dt. \tag{1}$$

Here r is the interest rate, which may not be constant. If the portfolio contains stock, the stochastic differential equation for the stock price S is

$$dS = rSdt + \sigma S dW_1, \tag{2}$$

where σ is the volatility of the price and W_1 denotes a Wiener process in the risk-neutral world. Since the interest rate may not be constant, we follow Björk [4] and assume that the dynamics of r is given by

$$dr = (a - \kappa r - \lambda_P \Sigma)dt + \Sigma dW_2. \tag{3}$$

Here $\bar{r}$ is is the long-term average value of the interest rate, κ denotes the reversion speed to the steady-state value of the interest rate, and $a = \kappa\bar{r}$. Additionally Σ measures the volatility of the stochastic rate change [9], λ_P is the market price of risk, and W_2 denotes a Wiener process in a risk free probability space. An ideally complete market is characterized by large κ which defines a fast mean-reverting environment. As κ decreases and Σ increases, the market is less complete with higher volatility in the interest rate fluctuations and a slower mean-reverting environment.

Further, the interest rate r may be written as the sum of a constant value, r_0, and a stochastic component $x(t)$

$$r = r_0 + x(t), \tag{4}$$

where $x(t)$ follows a decaying Ornstein-Uhlenbeck process. Also r_0 is not necessarily $\bar{r}$. Substituting (4) into (3) we find

$$dx = -\kappa x dt + r^{\beta}\Sigma dW_2. \tag{5}$$

For this paper we limit this decaying process to models of the form: $\beta = \frac{1}{2}$, $\lambda_P = \frac{\lambda_0\sqrt{r}}{\Sigma}$ in the CIR model, and $\beta = 0$, $\lambda_P = \lambda_0$ in the Vasicek model,

with λ_0 a (different) constant in both models [9]. The Vasicek model is chosen for its mathematical simplicity while the CIR model may be the most widely used model to price bond derivatives, by virtue that this model is designed to be consistent with the observed term structure of interest rates. Further, we follow Björk [4] and Rebonato [9] by setting $\kappa\bar{r} - \kappa r_0 - \lambda_0 \Sigma = 0$ in the Vasicek model and $\kappa\bar{r} - \kappa r_0 - \lambda_0 r_0 = 0$ in the CIR model. These assumptions define x to be mean reverting to zero. In other words the above formulation defines the variable x so that it fluctuates around zero before eventually decaying to zero. Hence, the Vasicek and CIR models impose an explicit mean-reverting drift to the short rate process. These assumptions may be satisfied by selecting appropriate values for r_0. For example in the Vasicek model we set $r_0 = \bar{r} - \dfrac{\lambda_0 \Sigma}{\kappa}$. Hence, r_0 represents an average value of the long term interest rate adjusted by the given market price of risk.

For a two-factor option pricing model with underlying variables S and r defined as above, if we assume there is no correlation between the two Wiener processes dW_1 and dW_2, one finds the generalized Black-Scholes PDE [6]

$$\frac{\partial V}{\partial t} + \frac{\sigma^2 S^2}{2}\frac{\partial^2 V}{\partial S^2} + S\frac{\partial V}{\partial S}r - rV + \frac{(\Sigma r^\beta)^2}{2}\frac{\partial^2 V}{\partial r^2} + \frac{\partial V}{\partial r}(a - \kappa r - \lambda_P \Sigma r^\beta) = 0, \tag{6}$$

for the option price V. For the Vasicek model [6] this PDE is

$$\frac{\partial V}{\partial t} + \frac{\sigma^2 S^2}{2}\frac{\partial^2 V}{\partial S^2} + S\frac{\partial V}{\partial S}(r_0 + x) - (r_0 + x)V + \frac{\Sigma^2}{2}\frac{\partial^2 V}{\partial x^2} - \kappa x\frac{\partial V}{\partial x} = 0. \tag{7}$$

For the Cox-Ingersoll-Ross model we find

$$\frac{\partial V}{\partial t} + \frac{\sigma^2 S^2}{2}\frac{\partial^2 V}{\partial S^2} + S\frac{\partial V}{\partial S}(r_0 + x) - (r_0 + x)V + \frac{\Sigma^2(r_0 + x)}{2}\frac{\partial^2 V}{\partial x^2} - \frac{a}{r_0}x\frac{\partial V}{\partial x} = 0. \tag{8}$$

These equations are subject to initial and boundary conditions. Generally speaking, derivative pricing models for different financial scenarios may share a similar pricing partial differential equation (PDE) with adjusted parameters and boundary conditions. For example, Moreno [7] used (7) and (8) to price the options on bonds with two-factor (Vasicek or CIR) models by defining market prices of spread and long-term risk. Barone-Adesi, Bermudez and Hatgioannides [2] solved a two-factor convertible bonds model with calibrated

parameters for their PDE. Hence, depending upon the boundary conditions one defines different portfolio compositions. We shall define boundary conditions examining stock and convertible bond portfolios. In this regard if the above equations are independent of S, then $V(S, x, t) = P(x, t)$ represents the price of a bond, see [12]. If the equations are independent of x, then we have the classical Black-Scholes equation for the price of an option in a constant interest rate scenario. We note that the models (7) and (8) reduce to the pure Black-Scholes analysis in the case of infinitely fast market reaction, i.e. $\kappa \to \infty$. The Black-Scholes model is also recovered when $x(t) \to 0$ and $\Sigma \to 0$.

Finally, the derivative price obtained by solving the PDE may be summed over the probability distribution of $x(t)$ to yield the expected price, as discussed in Section 4.

The remainder of this paper is organized as follows. Section 2 studies boundary conditions according to different portfolio models. Section 3 derives an exact solution to the Vasicek model over the domain $-r_0 \leq x \leq \infty$, and develops an exact solution for the price of bonds convertible to stock at expiration under a stochastic interest rate. The exact solutions are used to evaluate accuracy of the numerical simulation schemes. Sections 4 through 6 define the numerical simulation schemes to solve these models over the truncated domain of the independent variables, and present results of the simulations. For the numerical simulations the pricing solution is analyzed as the market completeness decreases from the ideal complete level to one with higher volatility of the interest rate and a slower mean-reverting environment. Simulations indicate that the CIR model yields more reasonable results than the Vasicek model in a less complete market.

2 Boundary Conditions

Boundary conditions defining two portfolios will be considered. The first set of conditions will describe a European call stock option. The second set of conditions models a convertible bond. The stock price S and interest rate fluctuation x, defined by the processes (2) and (5), can reach any position within their natural boundaries. As a result, the solution domain for the models is $-r_0 \leq x < \infty$, $0 \leq t \leq T$ and $0 \leq S < \infty$, where T is the expiration time. Notice that negative interest rates do not exist, which implies the instantaneous fluctuation $x(t)$ can not cross $-r_0$.

2.1 Boundary conditions for the stock option model

At the maturity time T, the call option price will be the payoff function

$$V(S, x, T) = \max(S - K, 0), \tag{9}$$

as is predefined at the beginning of writing the contract. Here S and V are in dollars, t is in years, and K is the strike price.

Putting the time element aside, we see there are four faces of the domain boundary box that need to be considered:

(1) At $S = 0$, the option is worthless:

$$V(0, x, t) = 0. \tag{10}$$

(2) At $S = S_{\max}$, with $S_{\max}$ large enough to reflect the behavior of the solution as $S \to \infty$, we will get a payoff $S(T) - K$ at expiration time T. The value at time t requires discounting back the strike price K and considering that the price at time t for the underlying asset is simply $S_{\max}$. Then a suitable boundary condition is

$$\begin{aligned} V(S_{\max}, x, t) &= S_{\max} - Ke^{-\int_t^T [r_0 + x(\tau)]\, d\tau} \\ &= S_{\max} - KP(x, t), \end{aligned} \tag{11}$$

in which the bond price $P(x, t)$ can be generated by solving (7) or (8) according to different interest rate models, with $P(x, T) = 1$.

(3) At $x = x_{\max}$, with $x_{\max}$ large enough to reflect the behavior of the solution as $x \to \infty$, the option value is assumed to be nearly linear with respect to price S because the bond value reduces to zero and so there is no discounting part. Hence the option price will be the underlying stock price only,

$$V(S, x_{\max}, t) = S. \tag{12}$$

(4) When $x \to -r_0$, some terms in (7) and (8) will disappear and some terms assume simpler forms. Thus the natural boundary condition at $x_{\min} = -r_0$ can be written as

$$\frac{\partial V}{\partial t} + \frac{\sigma^2 S^2}{2}\frac{\partial^2 V}{\partial S^2} + \frac{\Sigma^2}{2}\frac{\partial^2 V}{\partial x^2} - \kappa x \frac{\partial V}{\partial x} = 0 \tag{13}$$

for the Vasicek model and

$$\frac{\partial V}{\partial t} + \frac{\sigma^2 S^2}{2}\frac{\partial^2 V}{\partial S^2} - \frac{a}{r_0} x \frac{\partial V}{\partial x} = 0 \tag{14}$$

for the CIR model.

2.2 Boundary conditions for the convertible bond model

The price of a bond *that is convertible to stock just at expiration* can be solved for as a superposition of solutions to the general PDEs (7) or (8). By restricting the conversion to expiration only we avoid the free boundary problem for determining the location in (S, x, t) space that separates the holding region from the conversion region. In this case, the value of the bond may be written as a portfolio including long positions of one share of a call with strike price K, and K zero coupon bonds with \$1 payoff at maturity. Therefore, the value of the convertible bond is

$$V(S, x, t) = C(S, x, t) + KP(x, t), \tag{15}$$

where C is the value of the call option. If we remove any puttable and callable features for the convertible bond and assume unit conversion ratio, the terminal condition of such a convertible bond can be written as

$$\begin{aligned} V(S, x, T) &= \max(S - K, 0) + K \\ &= \max(S, K). \end{aligned} \tag{16}$$

This concurs with the result drawn by Bermudez and Nogueiras [3]. The boundary conditions for the convertible bond are analogous to what we have derived for the call option.

(1) At zero stock price $S = 0$, the convertible bond behaves like a zero-coupon bond that pays off $\$K$ when it matures. That is,

$$V(0, x, t) = KP(x, t). \tag{17}$$

(2) For large stock price $S_{\max}$, it is almost certain that the bond will be converted to one share of the stock. Hence

$$V(S_{\max}, x, t) = S_{\max}. \tag{18}$$

(3) When x is infinitely large, the bond component tends to zero. Since we do not enforce any time-dependent constraints of puttable and callable features, the upper bound and the lower bound to the price of the convertible bond are $\max(S, \infty)$ and $\max(S, 0)$ respectively. Therefore we define the boundary condition as

$$\begin{aligned} V(S, x_{\max}, t) &= \min(\max(S, \infty), \max(S, 0)) \\ &= \min(\infty, S) \\ &= S. \end{aligned} \tag{19}$$

(4) For a very small interest rate, instead of taking the homogeneous Neumann condition suggested by Bermudez and Nogueiras [3], the natural condition as defined in (13) or (14) will be used.

3 Exact Solutions for the Vasicek model

Otto [8] developed an exact solution to (7) subject to (9) - (12). That solution was not subject to any constraints at $x = -r_0$. Following Otto's approach and using the constraint (13) at $x = -r_0$ we find

$$V(S, x, t) = SN(d_1) - KP(x, t)N(d_2) \tag{20}$$

where

$$d_1 = \frac{\ln(S/K) - \ln(P(x,t)) + \hat{\sigma}^2(T-t)/2}{\hat{\sigma}\sqrt{T-t}}, \tag{21}$$

$$d_2 = d_1 - \hat{\sigma}\sqrt{T-t}, \tag{22}$$

$$\hat{\sigma}^2 = \sigma^2 + \Sigma^2, \tag{23}$$

and $N(y)$ is the cumulative normal distribution. The zero coupon bond pricing equation (7) in terms of Vasicek-like rates is

$$\frac{\partial P}{\partial t} - (r_0 + x)P + \frac{\Sigma^2}{2}\frac{\partial^2 P}{\partial x^2} - \kappa x \frac{\partial P}{\partial x} = 0. \tag{24}$$

The solution of (24) is of the form

$$P(x, t) = A(t, T)e^{-xB(t,T)} \tag{25}$$

subject to the final condition

$$P(x, T) = 1. \tag{26}$$

It is easily shown that

$$B(t,T) = \frac{1 - e^{\kappa(t-T)}}{\kappa} \tag{27}$$

and

$$\begin{aligned} A(t,T) = &\exp\{r_0(t-T) - \frac{\Sigma^2}{2\kappa^2}[(t-T) - \frac{2}{\kappa}(e^{\kappa(t-T)} - 1) \\ &+ \frac{1}{2\kappa}(e^{2\kappa(t-T)} - 1)]\} \end{aligned} \tag{28}$$

by substituting (25) into the bond pricing equation and solving for $A(t,T)$ and $B(t,T)$ separately. Equations (25), (27) and (28) yield the proper solution which emphasizes that the value at time t of a zero bond $P(x,t)$ depends only on the state variable $r = r_0 + x$, i.e. today's value of the short rate. It is instructive to verify that (20) satisfies the conditions (10) - (13). When $S \to 0$, d_1 and d_2 approach $-\infty$ which leads to zero values for $N(d_1)$ and $N(d_2)$, respectively. Thus $V(S,x,t) \to 0$. On the other hand, when $S \to \infty$, d_1 and d_2 also approach ∞. Now $N(d_1)$ and $N(d_2)$ approach one. Hence, the option value $V(S,x,t) = S_\infty - KP(x,t)$. For $x \to \infty$, the bond price $P(x,t) \to 0$ and thus d_1 and d_2 approach ∞. Hence the value for $V(S,x,t)$ is S as $x \to \infty$. As x approaches its lower bound $-r_0$, the natural boundary condition (13) is satisfied because (20) is clearly a solution of (7).

Notice that the bond equation (24) is a reduced equation for the option pricing equation (7) with S independence. Hence by the principle of linear superposition a portfolio with the value

$$\Pi(S,x,t) = nC(S,x,t) + \tilde{k}P(x,t) \tag{29}$$

is also a solution to (7). Here the call price $C(S,x,t)$ has strike price K/n and the solution for $C(S,x,t)$ is (20) with this strike price. If we assume the call and the bond expire at the same time T, the payoff function for the portfolio is

$$\begin{aligned} \Pi &= n\max(S - \frac{K}{n}, 0) + \tilde{k} \\ &= \max(nS - K, 0) + \tilde{k}. \end{aligned} \tag{30}$$

When $\tilde{k} = K$, (29) satisfies conditions (16) - (19) and we have the solution for a bond convertible to n shares of stock at expiration. This solution is valid for the Vasicek model. We shall obtain a solution numerically for the CIR model. The superposition solution (29) extends the analytical solution from Bermudez and Nogueiras [3]. The latter is only valid for constant interest rates.

4 Probability density functions

For the stochastic interest rate setting, the calculated solutions of (7) and (8) may be summed over the probability distribution of $x(t)$ to obtain the expected derivative price.

In order to derive a solution analogous to that for the Black-Scholes equation, we integrate the option price $V(S, x, t)$ over the risk-neutral probability distribution density for $x(t)$ appropriate to the Vasicek or CIR model. The expected option price can then be calculated as

$$\bar{V}(S,t) = \int_{-r_0}^{\infty} V(S,x,t)p(x_t = x|x_T = 0)\,dx, \tag{31}$$

where $p(x_t = x|x_T = 0)$ is the conditional probability density function for the interest rate fluctuation $x(t)$ given that its value is zero at maturity T. Considering the processes (5), with $\beta = 0$ or $1/2$ one can see that they are both mean-reverting to zero, which makes the explicit forms of transition probabilities attainable. In general for other interest models, an analytical solution for the distribution density function is almost impossible to find.

4.1 Probability distribution for the Vasicek model

As discussed by Otto [8], for a Vasicek-like process and given $x(0)$ the value $x(t)$ is normally distributed with mean $\mu = e^{-\kappa t}x(0)$ and variance $\sigma^2 = \frac{\Sigma^2}{2\kappa}(1 - e^{-2\kappa t})$. The transition probability density function is determined from the distribution

$$\begin{aligned} p(\tau, x(0), y)dy &= \frac{1}{\sqrt{2\pi\sigma^2}} e^{-\frac{(y-\mu)^2}{2\sigma^2}} dy \\ &= \frac{1}{\sqrt{\frac{\pi\Sigma^2}{\kappa}(1 - e^{-2\kappa\tau})}} e^{-\frac{\kappa}{\Sigma^2}\frac{(y - e^{-\kappa\tau}x(0))^2}{1-e^{-2\kappa\tau}}} dy, \end{aligned} \tag{32}$$

where τ is the time interval for the random variable x to reach the point y, starting from $x(0)$. Using this we follow Otto to define the backward transition probability $p(x_t = x|x_T = 0)$ to describe the probability of x at time t given that it will surely go to zero at time T.

4.2 Probability distribution for the CIR model

Since the transition probability is not directly available for $x(t)$ in the framework of the CIR model, we make a change of variables for $x(t)$ by letting $r = x(t) + r_0$ for positive values of r. Cox et al. [5] give the transition density function for r as

$$p(\tau, r(0), y)dy = ce^{-u-v}(\frac{v}{u})^{q/2}I_q(2\sqrt{uv})dy, \tag{33}$$

where $c = \frac{2\kappa}{\Sigma^2(1-e^{-\kappa\tau})}$, $u = cr(0)e^{-\kappa\tau}$, $v = cy$, $q = \frac{2\kappa r_0}{\Sigma^2} - 1$, and $I_q(\cdot)$ is the modified Bessel function of the first kind of order q. Cox notes that "r can reach zero if $\Sigma^2 > 2\kappa r_0$. If $2\kappa r_0 \geq \Sigma^2$, the upward drift is sufficiently large to make the origin inaccessible", i.e., x has zero probability to hit the boundary $-r_0$. The following solution procedure is based on the above condition $2\kappa r_0 \geq \Sigma^2$ to ensure that the spot rate stays positive. The transition density function is a non-central chi-square $\chi^2[2cy; 2q + 2; 2u]$ distribution with $2q + 2$ degrees of freedom and non-centrality parameter $2u$. If $\kappa > 0$, then as $t \to \infty$, its distribution will approach a Gamma distribution given by

$$\hat{p}(z) = \frac{1}{\Gamma(\alpha)\beta^\alpha}z^{\alpha-1}e^{-z/\beta}, \tag{34}$$

where $\alpha = 2\kappa r_0/\Sigma^2$ and $\beta = \Sigma^2/2\kappa$. This is a stationary distribution in the sense that if $x(0)$ is drawn from this distribution, then $x(t)$ has the same distribution for all t. To derive the "transition probability of interest" $p(r_t = x_t + r_0|r_T = r_0)$, we use Otto's approach

$$p(r_t = r_0 + x_t|r_T = r_0) = p(\tau, r(0), y)\frac{\hat{p}(r)}{\hat{p}(r_0)} \tag{35}$$

in which $\hat{p}(z)$ is the limit probability density for r as $t \to \infty$, i.e., the density function for the Gamma distribution. The final expression for the transition probability in the framework of the CIR model thus reads:

$$\begin{aligned} p(x_t = x|x_T = 0) &= p(r_t = r_0 + x_t|r_T = r_0) \\ &= ce^{-u-v}(\frac{v}{u})^{q/2}I_q(2\sqrt{uv})(1 + \frac{x}{r_0})^{\alpha-1}e^{-x/\beta} \end{aligned} \tag{36}$$

where $c = \frac{2(a/r_0)}{\Sigma^2(1-e^{-(a/r_0)(T-t)})}$, $u = c(x + r_0)e^{-(a/r_0)(T-t)}$, $v = cr_0$, $q = \frac{2a}{\Sigma^2} - 1$, $\alpha = 2a/\Sigma^2$, $a = \kappa\bar{r}$ and $\beta = \Sigma^2 r_0/2a$. Figure 1(a) compares the distributions of the CIR and Vasicek models. The comparison is based on $\kappa = 5$, $\Sigma = 0.2$, and $\tau = 0.8$. The figure suggests that the square-root diffusion in CIR gives a more

reasonable risk-neutral distribution for $x(t)$. The solid line shows the complete distribution of $x(t)$ while the dashed curve for the Vasicek process is truncated because negative short rates are not allowed. We can also see from Figure 1(b) that if the market is acting more "completely", i.e. with faster market reaction rate κ and lower volatility Σ of the interest rate fluctuation, the distributions for both diffusion processes are approaching the Dirac δ-function. This result is desirable since in an ideal complete market the integral over the entire spectrum of $x(t)$ should be exactly the option value at $x(t) = 0$, that is, the riskless rate r_0.

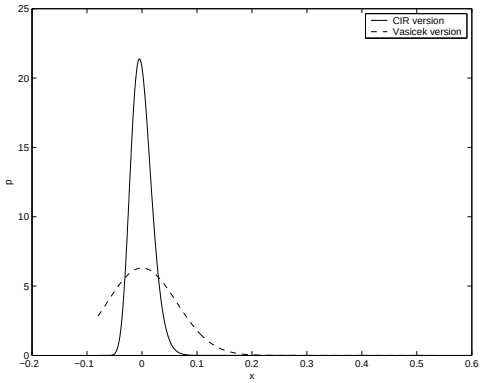

Fig.1(a): $\kappa = 5$ and $\Sigma = 0.2$ at $\tau = 0.8$ and $r_0 = 0.08$.

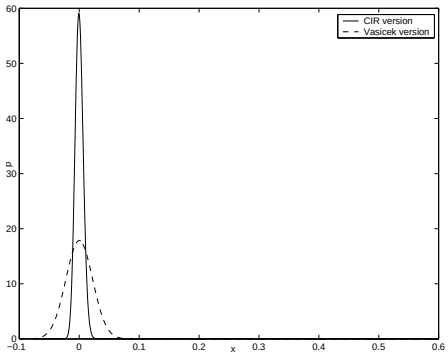

Fig. 1(b): $\kappa = 10$ and $\Sigma = 0.1$ at $\tau = 0.8$ and $r_0 = 0.08$.

Fig. 1. Comparison of probability distribution of CIR version (solid) and Vasicek version (dashed)

5 Numerical Schemes

Equations (7) and (8) can be written in the following general form

$$\frac{\partial V}{\partial t} + a(S,x,t)\frac{\partial^2 V}{\partial S^2} + b(S,x,t)\frac{\partial V}{\partial S} + c(S,x,t)V + d(S,x,t)\frac{\partial^2 V}{\partial x^2} + e(S,x,t)\frac{\partial V}{\partial x} = 0 \quad (37)$$

with terminal condition (9). By using $\tau = T - t$, we can rewrite (37) as

$$\frac{\partial V}{\partial \tau} = a(S,x,t)\frac{\partial^2 V}{\partial S^2} + b(S,x,t)\frac{\partial V}{\partial S} + c(S,x,t)V + d(S,x,t)\frac{\partial^2 V}{\partial x^2} + e(S,x,t)\frac{\partial V}{\partial x} \quad (38)$$

with initial condition

$$V(0) = max(S - K, 0). \tag{39}$$

We solve (38) with forward time-stepping using the up-wind Alternating Direction Implicit (ADI) scheme.

5.1 Implementation of boundary conditions

For boundary conditions (13) and (14), one way to simplify the computation is to completely ignore partial derivatives with respect to x. For comparison, we also use the one-sided finite difference to approximate the partial derivatives with respect to x, as suggested by Tavella and Randall [10], although they only applied it to a one-factor model. When the ADI method is applied to the two-factor model PDE, each time step progressing from t_k to t_{k+1}, involves two substeps. The partial derivatives with respect to x in (13) and (14) are treated implicitly in the first substep, i.e. proceeding from t_k to $t_{k+\frac{1}{2}}$, while those with respect to S are treated explicitly. In the second substep, i.e. proceeding from $t_{k+\frac{1}{2}}$ to t_{k+1}, the partial derivatives with respect to x in (13) and (14) are treated explicitly while those with respect to S are treated implicitly. The curves in Figure 2 represent different solutions to (7) subject to (9)-(12) with three different approximations for boundary condition (13): With both $\partial V/\partial x$ and $\partial^2 V/\partial x^2$, without the second derivative $\partial^2 V/\partial x^2$, and without any derivatives with respect to x. We plot the curves against the exact solution (20) (represented by the dashed line). It is clear from the figure that one cannot completely ignore partial derivatives with respect to x at the leftmost boundary $x = -r_0$. Even if we reduce the sizes of time and space grids, the solution without derivatives with respect to x does not converge to the exact solution. Another observation from Figure 2 is that the second derivative of x in the boundary condition does not affect the accuracy of the solution as significantly as does the first derivative. For the remainder of this study, we use the complete boundary condition (13) or (14) for better accuracy.

Another important issue that affects computational efficiency is the choice of S_{max} and x_{max} to reduce an infinite domain $[-r_0, \infty) \times [0, \infty)$ to a finite domain $[-r_0, x_{max}] \times [0, S_{max}]$ for numerical computations. There has been very little discussion about this in the existing literature. Since boundary conditions at x_{max} and S_{max} are derived to approximate the behavior as $x \to \infty$ and $S \to \infty$, it is obvious that larger x_{max} and S_{max} will provide better approximations. However this also means longer computing time since more grid points are needed to cover the larger computational domain. Our numerical experiments have indicated that using an S_{max} that is 2 to 2.5 times the strike price K usually provides adequate accuracy. For the x-dimension, however, there are

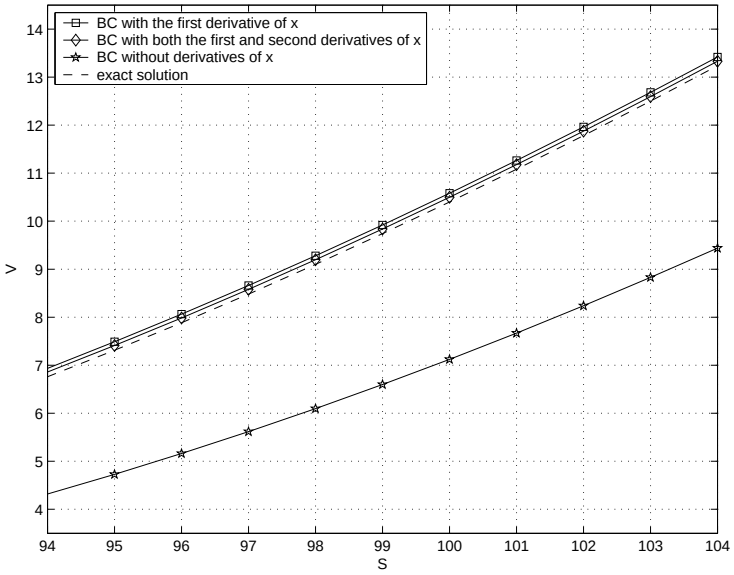

Fig. 2. Comparison of solutions with different boundary condition approximations with the exact solution (20) for $\Delta t = 0.001$, $\Delta x = 0.05$, $\Delta S = 1$. Parameters are: $T - \tau = 0.8$, $\sigma = 0.2$, $\Sigma = 0.8$, $\kappa = 100$ and $K = 100$.

two issues. One is the accuracy of the numerical solution of the model PDEs. Figure 3(a) shows that the bond price numerical solution with the Vasicek model, using $x_{max} = 50$, matches very well to the exact solution described by (25) until one or two grid points before x_{max}. At x_{max}, we observe a sudden jump at the end point to satisfy the boundary condition that the bond price reaches zero as $x \to \infty$. Figure 3(b) shows similar results for both the Vasicek and CIR models. This is typical in our numerical experiment, which indicates that the value of x_{max} does not affect the accuracy of the numerical solutions significantly.

The final issue is the accuracy of the option price after integrating the numerical solution with respect to x using the proper probability distribution. Since the normal distribution curve associated with the Vasicek model is very sensitive to parameters, we were unable to identify a clear correlation between x_{max} and the parameters. On the other hand, we noticed that for the CIR model, the chi-square distribution curve approaches zero near $x = 0.4\Sigma$. Hence $x_{max} \simeq 0.4\Sigma$ is usually adequate for the CIR model. The error caused by the jump near x_{max} is generally negligible since the probability distribution is almost zero there.

6 Numerical results

In Figure 4, the value of a European call option (with boundary conditions (9)-(14) and $K = \$50$) is shown as a function of both the underlying stock price

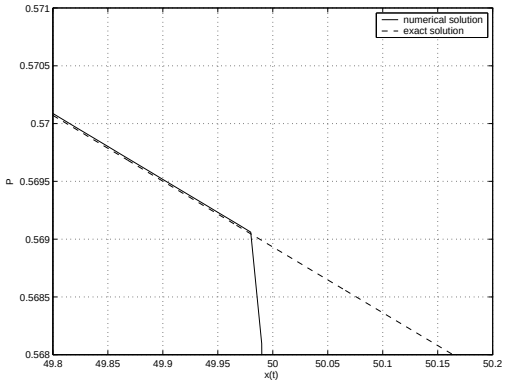

Fig. 3(a): Parameters: $\kappa = 100$ and $\Sigma = 0.4$ at $\tau = 0.8$. When $x(t)$ reaches its maximum 50, the solid line extends to zero.

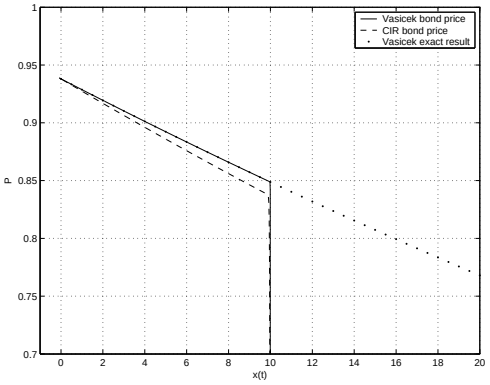

Fig. 3(b): Parameters: $\kappa = 200$ and $\Sigma = 0.4$ at $\tau = 0.8$. When $x(t)$ reaches its maximum value 10, both simulated yield curves reach zero. The exact solution of the Vasicek bond price is also shown (dotted).

Fig. 3. Comparison of numerical solution and the exact solution for the bondprice, near the truncated computational domain for $x(t)$.

and the instantaneous change of interest rate. The averaged price $\bar{V}$ is deter-

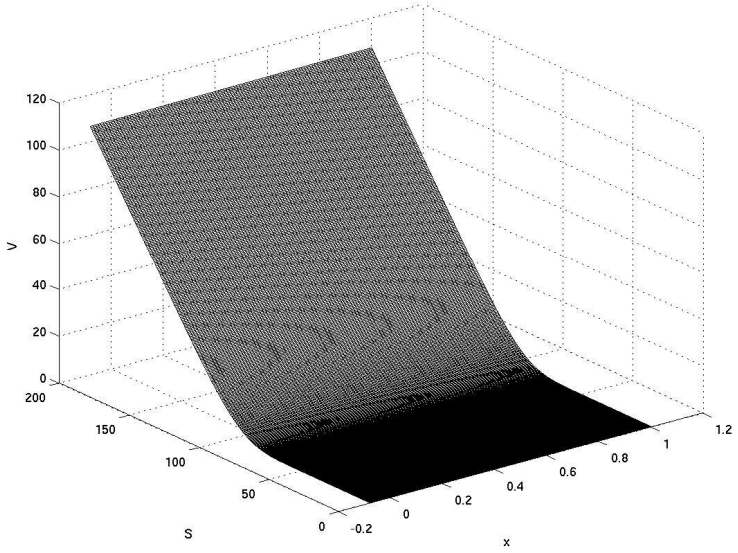

Fig. 4. The value of a call option as a function of asset S and x in the domain $[-0.08, 1]$ and $[0, 200]$ for x and S, respectively. Parameters: $\kappa = 100$, $r_0 = 0.08$, $\sigma = 0.2$ and $\Sigma = 0.4$ at $\tau = 0.8$.

mined by integrating over the probability density of the fluctuation $x(t)$. The results are shown in Figure 5(a). The trapezoid rule for numerical integration of (31) is applied for this purpose.

We relax the assumption of market completeness at different levels by reducing κ and increasing Σ, and compare the results with the standard Black-Scholes price with constant interest rate. The term *moneyness* $m = S/K$ is introduced as a measure of the degree to which a call option is likely to have monetary value. Figure 5(a) shows that, over a reasonable range of the moneyness $m \simeq 1$, the price of a European call option under the two frameworks of interest rate models is close to that from the Black-Scholes model. When the option is around the *at-the-money* ($m \simeq 1$) value, the curves for both models have a bell shape with averaged option values higher than that from the Black-Scholes model due to the stochastic interest rate. The option prices decrease as they go deep *in the money* ($m \gg 1$). The largest price difference between either model and the Black-Scholes model is around \$0.08. We comment that this small difference in price between the constant interest rate Black-Scholes model and the stochastic interest rate models is consistent with the empirical study of Bakshi, Cao and Chen [1]. That study demonstrated the small influence of fluctuations in the interest rate on option prices.

Now we examine the situation when the market becomes less "complete". Figures 5(b) 5(c) show the curves for both pricing models using the parameters $\kappa = 5$, $\Sigma = 0.2$ and $\kappa = 1$, $\Sigma = 0.8$, respectively. For both cases, the in-the-money range shows a serious mispricing in the Vasicek model. The option price decreases below the Black-Scholes price dramatically as the underlying stock price increases. As we see from Figure 5(a), the situation becomes even worse for lower κ and higher Σ. To give a clear illustration, Figure 6 shows a contour plot corresponding to unaveraged price differences for the same market as Figure 5(b). We see for small x that both models agree with the Black-Scholes price, whereas for larger x the models deviate from the Black-Scholes price. The close proximity of the contour levels for small x implies close agreement between the models. It further implies that the integration over the probability density causes the obvious difference in average price. As pointed out in the previous section, the limitation of $x \geq -r_0$ truncates the risk-neutral density function curve of the Vasicek model and makes it incomplete. Hence probability densities weighted on the negative interest rates will be lost if we increase the degree of market "incompleteness". This leads to nonzero probabilities of negative interest rates in the Vasicek model so that the averaged option is mispriced over a portion of the domain of x. On the other hand, the CIR model correctly captures the risk neutral distribution of interest rates and gives a more reasonable price curve in Figure 5(b). A similar mispricing also occurs in the CIR model in Figure 5(c) simply because the condition $2\kappa r_0 \geq \Sigma^2$ is violated. Figure 7(a) shows the result with fixed κ and decreasing Σ to prevent mispricing. The plot is similar to Figure 5(b). Therefore, the CIR model works well for small Σ. The difference between the call option averaged price from the CIR model and that from the Black-Scholes model at different times is given in Figure 7(b). Hence the results approach V_{B-S} as $t \to T$, since x decays to 0.

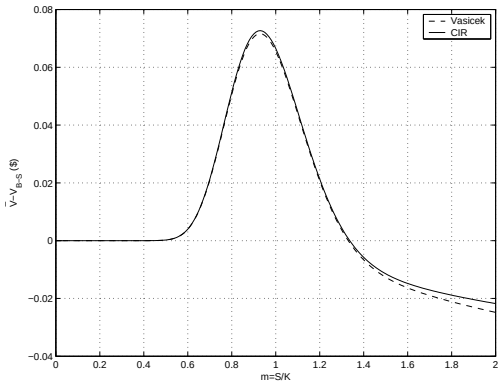

Fig. 5(a): Parameters: $\kappa = 10$, $r_0 = 0.08$, $\bar{r} = 0.07$, $\sigma = 0.2$ and $\Sigma = 0.1$ at $\tau = 0.8$.

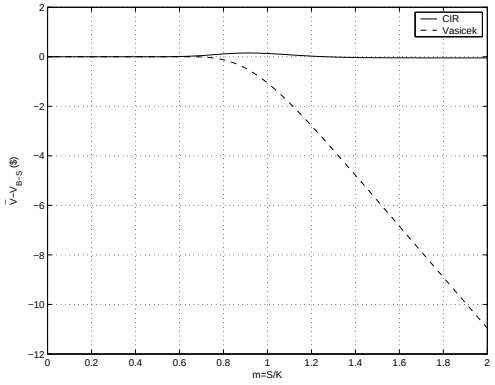

Fig. 5(b): Parameters: $\kappa = 5$, $r_0 = 0.08$, $\bar{r} = 0.07$, $\sigma = 0.2$ and $\Sigma = 0.2$ at $\tau = 0.8$.

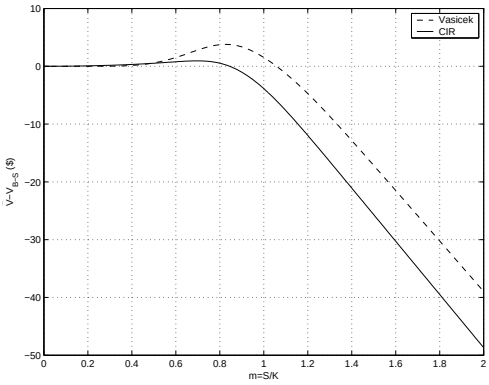

Fig. 5(c): Parameters: $\kappa = 1$, $r_0 = 0.08$, $\bar{r} = 0.07$, $\sigma = 0.2$ and $\Sigma = 0.8$ at $\tau = 0.8$.

Fig. 5. Difference between the call option price and the Black-Scholes value as a function of moneyness $m = S/K$, for the yield curves of the Vasicek process and the CIR process.

Consider the convertible bond portfolio discussed in Section 2.2. To validate the accuracy of our numerical solution Figure 8(a) is a contour plot of the difference in value with (29) for $n = 1$, $\tilde{k} = K$ and the numerical solution for the Vasicek model. The contour plot of the difference in value between the Vasicek and CIR models is shown in Figure 8(b). With increasing x or S, the difference is increasing.

We have shown that the stochastic interest rate model using the CIR process outperforms the Vasicek model in accurately describing the risk-neutral distribution of interest rates. The CIR model nicely produces the price curve without losing the general characteristics of fluctuating interest rates, provided that $2\kappa r_0 \geq \Sigma^2$. However, in the Vasicek model, serious mispricing could take

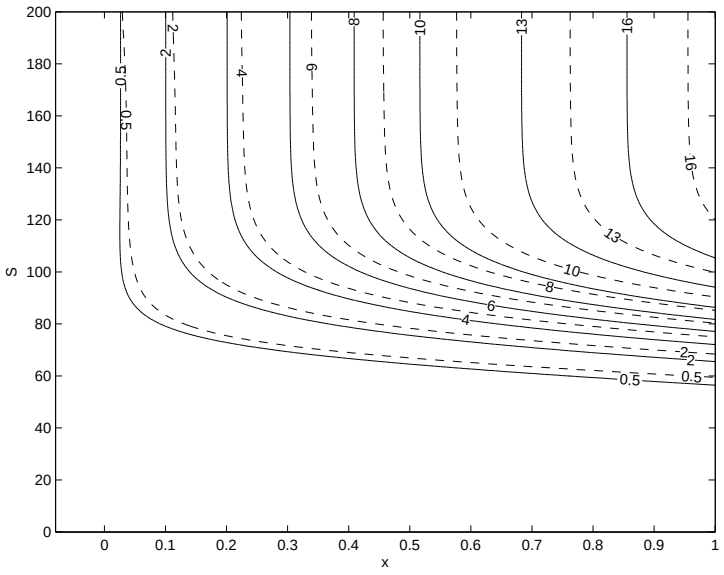

Fig. 6. Contour plots of the difference in price $(V(S,r,t) - V_{B-S})$ for the Vasicek model (dashed line) and the CIR model (solid line) on $S - x$ surface. Parameters: $\kappa = 5$, $r_0 = 0.08$, $\bar{r} = 0.07$, $\sigma = 0.2$ and $\Sigma = 0.2$ at $\tau = 0.8$.

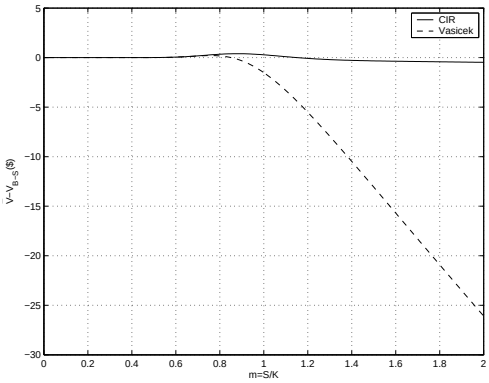

Fig. 7(a): Parameters: $\kappa = 1$, $r_0 = 0.08$, $\bar{r} = 0.07$, $\sigma = 0.2$ and $\Sigma = 0.2$ at $\tau = 0.8$ (For CIR process only, at different time frames).

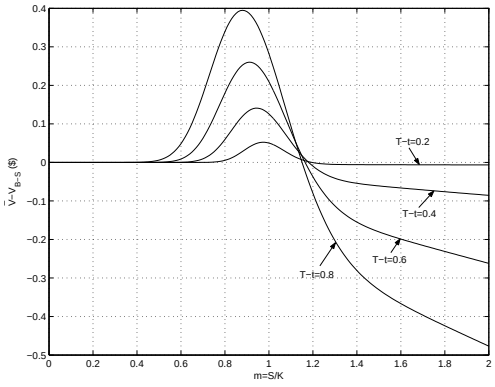

Fig. 7(b): Parameters: $\kappa = 1$, $r_0 = 0.08$, $\bar{r} = 0.07$, $\sigma = 0.2$ and $\Sigma = 0.2$.

Fig. 7. Difference between the call option price and the Black-Scholes value as a function of moneyness $m = S/K$, for the yield curves of the Vasicek process and the CIR process.

place when the market becomes less complete.

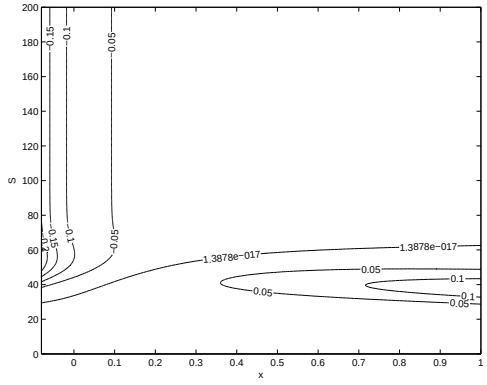

Fig.8(a): Contour plot of the difference in value with (29) for $n = 1$, $\tilde{k} = K$ and the numerical solution for the Vasicek model. Parameters: $\kappa = 5$, $r_0 = 0.08$, $\bar{r} = 0.07$, $\sigma = 0.2$, $\Sigma = 0.2$ at $\tau = 0.8$, $dt = 0.001$, $dS = 0.5$ and $dx = 0.01$.

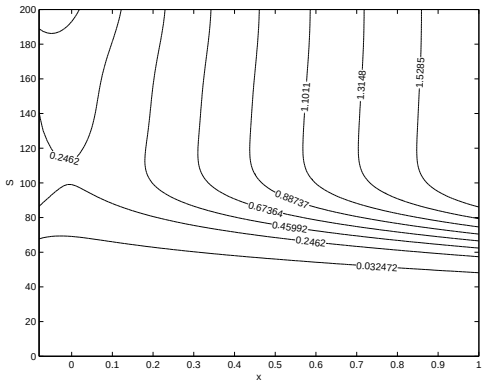

Fig. 8(b): Contour plot of the difference in value between the portfolios with the Vasicek model and the CIR model. Parameters: $\kappa = 5$, $r_0 = 0.08$, $\bar{r} = 0.07$, $\sigma = 0.2$ and $\Sigma = 0.2$ at $\tau = 0.8$.

Fig. 8. Contour plots.

7 Summary

The basic idea of pricing is to determine the risk neutral distribution of the underlying assets. One approach is to solve the pricing PDE (for example, Black-Scholes PDE, (7) and (8) etc.) according to different models. Another nontrivial approach is to simulate the sample paths by using Monte Carlo simulation, especially in the case that the probability distribution of $x(t)$ is not known. Such a simulation method is commonly used in practice because only a limited number of models come with the exact risk-neutral distribution. The Vasicek and CIR models are in that small pool.

Hence, taking advantage of the exact distributions, we presented and solved models for stochastic interest rates in an incomplete market. We have shown that the CIR type model for the interest rate fluctuation gives a better result than the Vasicek model by preventing mispricing. In summary this paper:

- formulates stochastic interest rate models based on the CIR and Vasicek processes,
- specifies the boundary conditions for models in Section 2,
- develops numerical schemes to solve these models over the truncated domains of the independent variables,
- shows that the CIR model yields more reasonable results than the Vasicek model in a less complete market,
- determines an analytical expression of the solution to the Vasicek model

over the domain $-r_0 \leq x \leq \infty$ in Section 3,

- develops an exact solution for the price of bonds convertible to stock at expiration, and under a stochastic interest rate in Section 3.

References

[1] G. S. Bakshi, C. Cao, and Z. Chen, *Empirical performance of alternative option pricing models*, Journal of Finance, 52 (1997), pp. 2003–2049.

[2] G. Barone-Adesi, A. Bermudez, and J. Hatgioannides, *Two-factor convertible bonds valuation using the method of characteristics/finite elements*, Journal of Economic Dynamics and Control, 27 (2003), pp. 1801–1831.

[3] A. Bermudez and M. R. Nogueiras, *Numerical solution of two-factor models for valuation of financial derivatives*, Mathematical Models and methods in Applied Sciences, 14 (2004), pp. 295–327.

[4] T. Björk, *Arbitrage Theory in Continuous Time*, Oxford University Press, 1st ed., 1999.

[5] J. Cox, J. Ingersoll, and S. Ross, *A theory of the term structure of interest rates*, Econometrica, 58 (1985), pp. 385–407.

[6] J. C. Hull, *Options, Futures, and Other Derivatives*, Prentice Hall, 5th ed., 2003.

[7] M. Moreno, *A two-mean reverting-factor model of the term structure of interest rates*, The Journal of Future Markets, 23 (2003), pp. 1075–1105.

[8] M. Otto, *Towards non-equilibrium option pricing theory*, The European Physical Journal B, 14 (2000), pp. 383–394.

[9] R. Rebonato, *Interest-Rate Option Models*, John Wiley and Sons, 2st ed., 1998.

[10] D. Tavella and C. Randall, *Pricing Financial Instruments: The Finite Difference Method*, Wiley, 1st ed., 2000.

[11] O. Vasicek, *An equilibrium characterization of the term structure*, Journal of Financial Economics, 5 (1977), pp. 177–188.

[12] P. Wilmott, S. Howison, and J. Dewynne, *The Mathematics of Financial Derivatives - A student Introduction*, Cambridge University Press, 1995.